Heliyon 7 (2021) e08345

Contents lists available at ScienceDirect

Heliyon

journal homepage: www.cell.com/heliyon

Research article

Impact of identical digital elevation model resolution and sources on morphometric parameters of Tena watershed, Ethiopia

Tesfu Abebe Tesema *

Department of Water Resources and Irrigation Engineering, Jigjiga University, Jijiga, Ethiopia

ARTICLE INFO

Keywords:
DEM
Morphometry
$SRTM_{30m}$
$ASTER_{30m}$
$ALOS_{30m}$
Tena watershed

ABSTRACT

Digital elevation models (DEMs) are the primary form of satellite data used to design and analyze the hydrology and hydraulic behavior of watersheds for water resource development. The primary objective of this study is to conduct morphometric parameter analysis using $SRTM_{30m}$, $ASTER_{30m}$, and $ALOS_{30m}$ data to determine the impact of identical DEM resolution and DEM sources on the Tena watershed by computing the basic and derived parameters. In this study I used data from two sources for morphometric parameter analysis with ArcGIS software. The results indicate that the DEM sources did not provide similar results for all parameters: $ASTER_{30m}$ was the maximum output for almost all parameters, followed by $SRTM_{30m}$ and $ALOS_{30m}$. The findings of this study suggest that $ASTER_{30m}$ is the most suitable data source for flood risk assessment, soil erosion, sediment, streamflow, and other watershed modelling, while $ALOS_{30m}$ is best suited for peak discharge analysis. All of the used DEM sources were suitable for computing watershed shape parameters. In general, the resolution of DEMs impacts the hydrological and hydraulic study of any watershed, with resulting effects on decision-making for watershed management and development.

1. Introduction

Digital elevation models (DEMs) are an important form of satellite or remote sensing data used in hydrological, hydraulic, climate change, agricultural management, and water resources development studies (Guiamel and Lee, 2020). The sources and resolution of DEMs impact the results obtained from hydraulic and hydrology models (Ali et al., 2015). For example, flood inundation mapping of river channels was affected by DEM sources (Williams et al., 2000; Dodov and Foufoula-Georgiou, 2006; Nardi et al., 2006) and the hydrological modelling of a watershed using the so-called Soil and Water Assessment Tool was influenced by DEM sources and resolution (Lin et al., 2010; Tan, M.L., Ramli, H.P. & Tam, T.H., 2018; Ficklin et al., 2013). Furthermore, DEMs have been frequently used for morphometric analysis of river basins by extracting topographic parameters such as stream networks that can be derived from flow directions and flow accumulations (Vaze et al., 2010; Ariza-Villaverde et al., 2015). A DEM is a regular gridded matrix representation of the land surface, including various topographical features, over time and space (Burrough, 1986). The fundamental features of any DEM data are accuracy and resolution (Sefercik and Alkan, 2009). Ghumman et al. (2017) tested the DEM efficiency at lower and higher resolution for a large (100 km2) area of the watershed; according to his report, the efficiency was similar for both tested resolution levels. However, for a smaller watershed of less than $1km^2$, researchers found that model efficiency was affected by DEM resolution for flood risk analysis and drainage pattern mapping (Sampson et al., 2015 and Woodrow et al., 2016).

The sources and accuracy of DEMs also impact morphometric parameter analysis, even for DEMs with identical resolution (Weydahl et al., 2007; Cook et al., 2012). Niyazi et al. (2019) used DEMs such as the Shuttle Radar Topographic Mission ($SRTM_{30m}$), the Advanced Space borne Thermal Emission and Reflection and Radiometer ($ASTER_{30m}$), and the Advanced Land Observation System (ALOS) (Takaku et al., 2014) ($ALOS_{30m}$) and found that the morphometric parameter results differed, with the exception of some parameters. During morphometric parameter analysis, Niyazi et al. (2019) found that stream order and stream length were the main controlling parameters. According to the authors, these parameters are reported in different result outputs for each DEM type. However, this study also stated that $SRTM_{30m}$ and $ASTER_{30m}$ provide closer morphometric parameters. These types of DEM data have also been used by other researchers; for example, $ASTER_{30m}$ (Evangelin et al., 2015), $SRTM_{30m}$ (Choudhari et al., 2018), and $ALOS_{30m}$ (Bayik et al., 2018).

* Corresponding author.
E-mail address: tesfuabebe@gmail.com.

https://doi.org/10.1016/j.heliyon.2021.e08345
Received 8 January 2021; Received in revised form 11 May 2021; Accepted 4 November 2021

Morphometric parameter analysis plays a significant role in understanding watersheds, including erosion characteristics, flood conditions, sediments, and runoff behavior. For instance, authors have computed morphometric parameters using ArcGIS software and mathematical equations in order to analyze linear, areal, and relief aspects of Earth's surface with the use of DEM data from different sources with the same resolution, or the same sources with different resolutions (Niyazi et al., 2019; Rai et al., 2014). The results of morphometric watershed parameters can be used directly or indirectly to prioritize sub-watersheds for forms of watershed management, such as soil conservation practice (Abdeta et al., 2020; Evangelin et al., 2015; Waiyasusri and Chotpantarat, 2020).

DEMs obtained from various sources with the same spatial resolution can be used to compare morphometric parameters. Such comparisons have been studied in Ethiopia (Abdeta et al., 2020; Gebre et al., 2015; Ayele et al., 2017; Gizachew and Berhan, 2018; Gutema et al., 2017) and worldwide (Aparna et al., 2015; Farhan 2017; Farhan et al., 2017; Javed et al., 2009; Jothimani et al., 2020; Kulkarni, 2013; Pande and Moharir, 2017; Prakash et al., 2016; Rai et al., 2014; Singh et al., 2014; Soni, 2017). Through morphometric parameter analysis, researchers can understand the specific areas of land degradation, flood risk, and surface water potential.

The primary objective of this study is to conduct morphometric parameter analysis using $SRTM_{30m}$, $ASTER_{30m}$, and $ALOS_{30m}$ to determine the impact of identical DEM resolutions and DEM sources on the Tena watershed by computing parameters of the linear, areal, and relief aspects.

2. Materials and methods

2.1. Study area

The Tena watershed is part of the Wabi Shebele river basin, situated in Tena *woreda*, Arsi Zone, Oromia Regional State of Ethiopia (Figure 1). The altitude of this *woreda* ranges from 1333 to 4185 m above sea level, with the highest point at Mount *Bada* (4195 m). Multiple rivers flow through the Tena watershed throughout the year, including the *Demasho*, *Hararghe, Serbona, and Walkesa* (near Ticho). The Tena *woreda* consists of agricultural land, swamps, and mountainous areas. In this study, the Tena watershed is sub-divided into 12 sub-watersheds (SWs) (Figure 1).

2.2. Data source

In this study, I used data downloaded from three freely available DEM sources: $ALOS_{30m}$, produced by the Japan Aerospace Exploration Agency (JAXA); $SRTM_{30m}$; and $ASTER_{30m}$.

2.3. Methods

Through the flowchart shown in Figure 2, in this study I aim to compute the major morphometric parameters of the Tena watershed using three types of DEM. I projected and extracted each DEM in the ArcGIS environment for further analysis to produce basic and derived parameters. Data errors were removed from the DEMs using the filling function tool in ArcGIS (Figure 2) to ensure proper stream network connectivity (Das et al., 2016). Errors may be depressions, pits, or sinks caused by data sampling elevations to integer numbers (Metz et al., 2011). I used the filled DEMs to generate natural water flows by utilizing the flow direction function (Figure 2). Flow accumulation is a fundamental tool to create stream networks, stream order, snap pour points, and the watershed outlet based on the raster calculator. I then subdivided the sub-watersheds using the snap pour points assigned at each joining stream network (Figure 2).

The basic parameters implemented in this study are as follows; sub-watershed area (A), sub-watershed perimeter (P), sub-watershed length (L_b), sub-watershed relief (B_h), stream order (S_o), stream number (S_n), and total stream length (Horton, 1945).

The derived parameters categorized as linear features (Horton, 1945; Schumm, 1956 and Faniran, 1968). Parameters classified as linear features have been studied by various researchers (e.g., Jasmin and Mallikarjuna, 2013). The identified relief features are relief ratio, relative relief, and the ruggedness number. These morphometric parameters have also been studied worldwide by Farhan and Nawaysa (2015) and Patton and Baker (1976), for instance. Areal aspects include the circulatory ratio (Miller, 1953), elongation ratio (Schumm, 1956), form factor (Horton, 1945), Lemniscate's ratio (Chorley et al., 1957), compactness coefficient

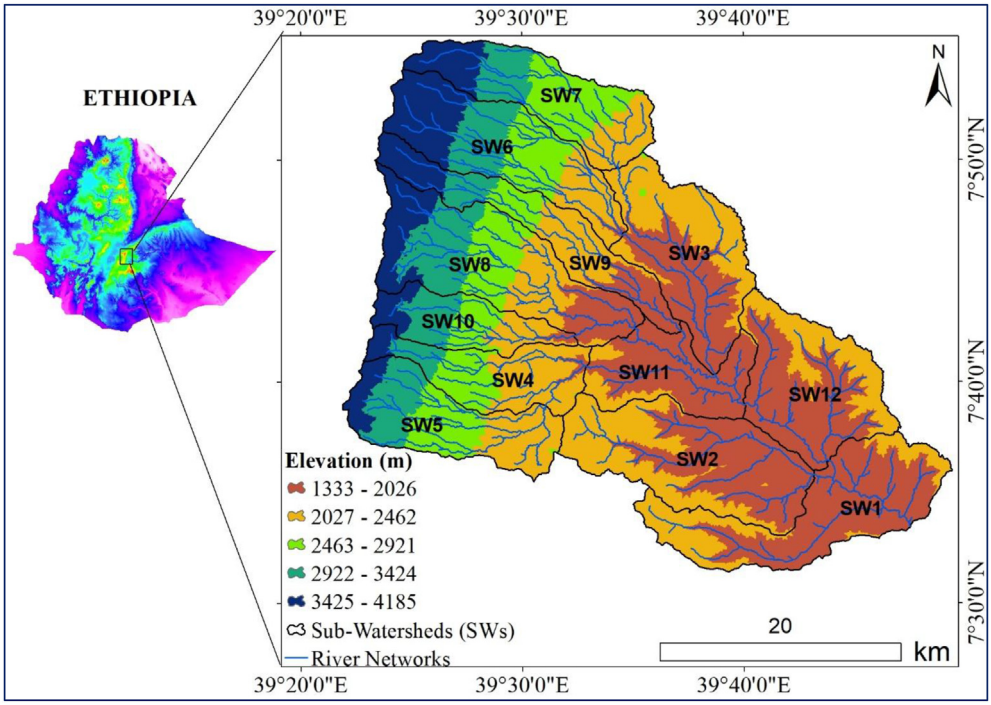

Figure 1. Map of the study area: the Tena watershed.

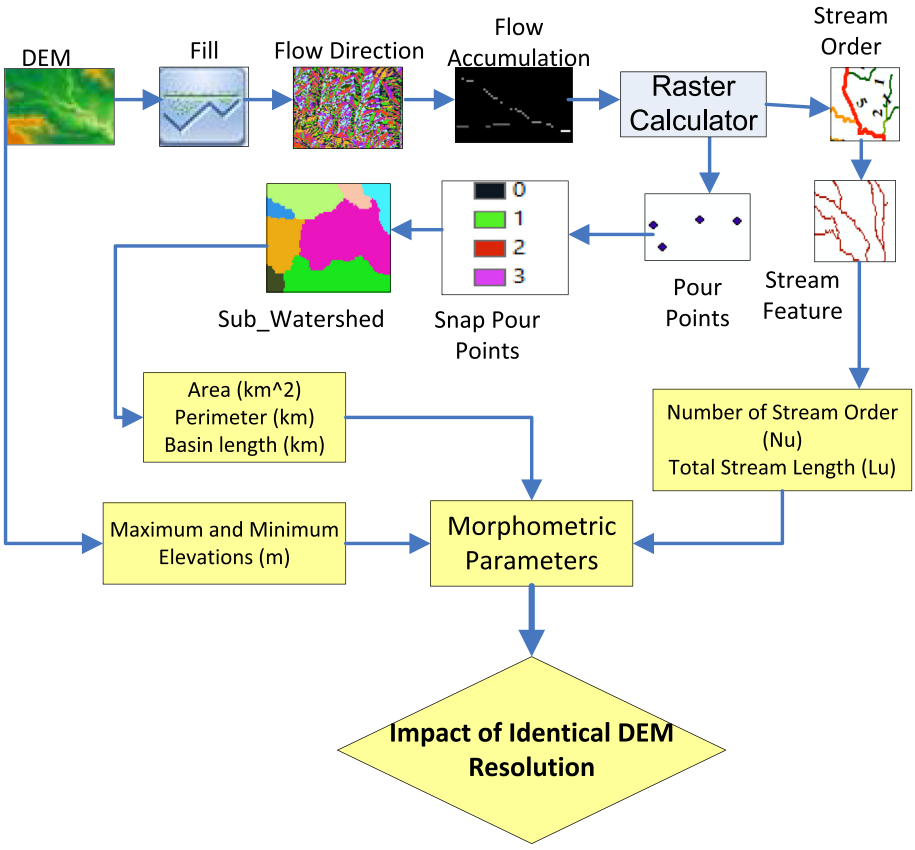

Figure 2. Morphometric parameter analysis flowchart.

(Horton, 1945), and the hypsometric integral (Strahler, 1952)). This study computes Tena watershed parameters derived from $ASTER_{30m}$, $SRTM_{30m}$, and $ALOS_{30m}$ (Table 1).

3. Results and discussion

3.1. Implication of DEMs for watershed area

Table 2 presents the variation in total area for each type of DEM in general, and particularly for sub-watershed area. The area (km^2) of a watershed or sub-watershed directly affects its hydrological water balance (Munoth and Goyal, 2019).

Additionally, Table 2 reports that the maximum area of the sub-watershed is SW_2 for $ALOS_{30m}$, and SW_8 for $ASTER_{30m}$ and $SRTM_{30m}$. $ASTER_{30m}$ indicates the largest total area of the watershed, followed by $SRTM_{30m}$ and $ALOS_{30m}$. These differing areas, calculated from data with equal DEM resolutions and different data sources, have impacts on the hydrological responses to stream discharge (Her et al., 2015). A larger area of the watershed implies smaller stream networks and a shorter time to generate stream lines. Meanwhile, an increasing number of stream networks implies increased peak flow from each hydrological response unit based on the intensity and distribution of precipitation. Moreover, the volume of water at the outlet of the watershed, or at other locations in the watershed and/or sub-watershed, is directly related to the area (Liebe et al., 2005). Hydrologically, a larger watershed or sub-watershed produces less runoff and evapotranspiration; however, DEMs in general shows a minor influence (Zhang et al., 2014; Tan et al., 2018). For instance, meteorological variables have greater influence on runoff estimation (Ekwueme and Agunwamba, 2020). Accordingly, SW_2 for $ALOS_{30m}$, and SW_8 for $ASTER_{30m}$ and $SRTM_{30m}$ produce the smallest amount of runoff and evapotranspiration (Table 2). As shown in Table 2, the total watershed area is largest for $ASTER_{30m}$ compared to the other DEM sources. Flood forecasting and sedimentation are directly related to the threshold area of the watershed and DEM resolution (Schumann et al., 2008; Munoth and Goyal, 2019). According to the $ASTER_{30m}$ DEM source, the Tena watershed exhibits a maximum area of 145.46 km^2 at the sub-watershed level and 1318.7 km^2 at the watershed level.

Figure 3 illustrates that different DEM sources provide different values of minimum and maximum elevation. Differences in elevation influence the climate characteristics of a watershed, the time of concentration, flood events, soil erosion, and flow discharge.

Stream orders are the fundamental parameters of watershed stream networks used to calculate other parameters, such as the bifurcation ratio. Denser stream orders are found upstream in a watershed, with sparser stream orders found downstream (Figure 4). As such, the calculated stream order is affected by DEM source.

Stream length (L_u) is the most significant morphometric parameter of a watershed. I computed the stream length of all sub-watersheds based on the law proposed by (Horton, 1945). The stream length of the Tena watershed is listed per sub-watershed for each DEM in Table 2. Longer stream lengths imply a flatter slope, while shorter stream lengths feature steeper slopes (Strahler, 1952; Sreedevi et al., 2005). Well drained watersheds with permeable bedrock tend to produce a longer stream length (Sethupathi et al., 2011). In the Tena watershed, SW_6, SW_5, and SW_8 are reported for $ALOS_{30m}$, $ASTER_{30m}$, and $SRTM_{30m}$, respectively, as maximum L_u (Table 2). These sub-watersheds are found upstream of the mountainous area of the Tena watershed (Figure 3). Based on Table 2, the maximum drainage length of the watershed is observed at SW_5 of L_u 131.25 km according to $ASTER_{30m}$. Regarding streamflow and water movement analysis, $ASTER_{30m}$ is well suited for the Tena watershed. Conversely, SW_{10} reports low values of L_u for all DEM types; but $ALOS_{30m}$ has the lowest L_u values, followed by $ASTER_{30m}$ and $SRTM_{30m}$ (Table 2). In summary, for sedimentation, soil erosion, and flooding studies $ALOS_{30m}$ is the optimal DEM for the Tena watershed.

Table 1. Formulae and methods used to compute watershed morphometric parameters.

Parameters	Formulae/Methods	Unit
Watershed area (*A*)		km^2
Watershed perimeter (*P*)		km
Maximum elevation (*H*)		m
Minimum elevation (*h*)		m
Stream order		Dimensionless
Basin length (L_b)	$L_b = 1.312A^{0.568}$	m
Stream number (N_u)	$N_u = N_{u1} + N_{u2} + N_{u3} + \ldots N_{un}$	Dimensionless
Stream length (Lu)	$L_u = L_{u1} + L_{u2} + L_{u3} + \ldots L_{un}$	km
Mean stream length (*Lsm*)	Average of stream length of all orders	km
Bifurcation ratio (R_b)	$R_b = N_u/N_{u+1}$	Dimensionless
Stream length ratio (R_l)	$R_l = L_u/L_{u-1}$	Dimensionless
Mean bifurcation ratio (R_{bm})	Average of bifurcation ratios of all orders	Dimensionless
Mean stream length ratio (R_{lm})	Average of bifurcation ratios of all orders	Dimensionless
Stream frequency (F_s)	$F_s = N_u/A$	km^{-2}
Drainage density (D_d)	$D_d = L_u/A$	km^{-1}
Drainage texture (D_t)	$D_t = N_u/P$	km^{-1}
Length of overland flow (L_o)	$L_o = 1/2D_d$	km
Drainage intensity (Di)	$D_i = F_s/D_d$	km^{-1}
Hydrologic coefficient (ρ)	$\rho = R_{lm}/R_b$	Dimensionless
Infiltration number (I_f)	$I_f = F_s{*}D_d$	km−3
Basin relief	$B_h = H_{max} - H_{min}$	km
Relief ratio (R_r)	$R_h = B_h/L_b$	Dimensionless
Relative relief (R_{hp})	$R_{hp} = H{*}1000/P$	Dimensionless
Ruggedness number (R_n)	$R_n = B_h{*}D_d$	Dimensionless
Circulatory ratio (R_c)	$R_c = 4\pi A/P^2$	Dimensionless
Elongation ratio (R_e)	$R_e = 2{L_b}^{-1}\sqrt{A/\pi}$	Dimensionless
Form factor (F_f)	$F_f = A{*}{L_b}^{-2}$	Dimensionless
Lemniscate's ratio (K)	$K = L_b^2/4A$	Dimensionless
Compactness coefficient (C_c)	$C_c = P/2\sqrt{A/\pi}$	Dimensionless

3.2. Derived parameters

Bifurcation ratios are morphometric parameters that are fundamental descriptors of the hydrological characteristics of any watershed. Increased flood damage and risk are indicated by a larger magnitude of the bifurcation ratio (McCullagh, 1978). The probability of flooding is higher for SW_6 according to all DEM sources (Figure 5); however, $SRTM_{30m}$ is preferable among the DEM sources for flood forecasting for the Tena watershed. Similar studies report direct links between the bifurcation ratio and flash flooding (Rakesh et al., 2000). Concerning sources of DEM analysis for flood risk, prediction, and inundation mapping, the SRTM DEM source is considered as the preferred estimator over the other DEM sources.

The hydrologic coefficient (ρ), stream frequency (F_s), and drainage density (D_d) are interconnected with the geologic, climatic, erosion, sedimentation, runoff, and infiltration characteristics of watershed hydrologic and hydraulic behaviors (Horton, 1945; Mesa, 2006; Sreedevi et al., 2005; Prasad et al., 2008; Ijam and Tarawneh, 2012 and Kaliraj et al., 2015). The maximum and minimum ρ values for the Tena watershed were found using $ASTER_{30m}$ for SW_{11} and SW_3, respectively (Figure 6). A higher ρ value indicates stable storage capacity during flooding events and erosion during high levels of discharge. It has been suggested that $ASTER_{30m}$ is optimal for storage capacity design among the DEM sources used in this study (Mesa, 2006).

The stream frequency of the watershed is an indicator of hydrogeological behavior, for example that of groundwater. Indeed, Fs and groundwater potential are directly related (Farhan and Al-Shaikh, 2017). In this study, watershed Fs ranges from 0.25 to 0.44/km^2 for $ALOS_{30m}$, 0.21 to 0.39/km^2 for $ASTER_{30m}$, and 0.26 to 0.43/km^2 for $SRTM_{30m}$ (Figure 6). For the purposes of groundwater potential analysis, recharge estimation, and groundwater quality assessment, the DEM source of $ALOS_{30m}$ is considered a good performance indicator.

Drainage density refers to the intricacy of arrangement of stream networks, and is used as a measure of the topographic partition and runoff potential of a specific watershed. A higher D_d value implies higher runoff, and consequently a lower infiltration rate (Prasad et al., 2008). For the Tena watershed, SW_6 provides the highest and nearly equal D_d value for all DEMs (Figure 6). Therefore, this sub-watershed is assumed to yield high runoff with low infiltration; it also features the high resistance of underground materials to erosion (Sahu et al., 2017). Figure 6 reports a low D_d value for SW_1, so this sub-watershed is characterized as high infiltration with low runoff (Prasad et al., 2008).

The basin relief (B_h), relief ratio (R_r), and ruggedness number (R_n) are morphometric parameters of a watershed while R_r and R_n dimensionless. These parameters are related to erosion, sediment yield, and flooding (Farhan and Nawaysa, 2015; Patton and Baker, 1976). As shown in Figure 7, the maximum B_h and R_n values are obtained for all DEM sources. The maximum B_h value is returned by $SRTM_{30m}$ for SW_9, followed by $ASTER_{30m}$ for SW_6, at the Tena watershed. Meanwhile, maximum R_n was found by $ASTER_{30m}$ for SW_6, followed by $SRTM_{30m}$ for SW_9. The other parameter presented in Figure 7 is R_r, which returns the same values for all DEM sources. The maximum values of the parameters

Table 2. Basic parameters of area (A), perimeter (P), basin length (L_b), and maximum stream order (U).

DEM		ALOS		ASTER		SRTM		ALOS	ASTER	SRTM
Parameters		A	P	A	P	A	P	L_b	L_b	L_b
Sub-Watersheds (SW)	SW_1	133.05	76.06	133.09	76.61	133.31	77.8	21.11	21.11	21.13
	SW_2	144.1	61.08	143.95	61.9	143.86	62.64	22.07	22.07	22.06
	SW_3	119.08	57.82	121.09	61.59	121.62	57.91	20.01	20.01	20.05
	SW_4	74.18	50.76	73.45	52.77	74.06	52.04	15.06	15.06	15.13
	SW_5	96.22	51.91	144.38	64.35	125.09	58.96	22.11	22.11	20.38
	SW_6	118.05	58.96	117.88	60.59	117.6	59.93	19.7	19.7	19.68
	SW_7	99.24	55.38	108.99	59.21	100.63	56.12	18.84	18.84	18.01
	SW_8	143.96	69.2	145.46	71.42	144.48	71.18	22.2	22.2	22.12
	SW_9	82.53	69.73	81.05	71.27	81.92	70.74	15.93	15.93	16.02
	SW_{10}	56.85	43.79	56.74	43.91	56.98	44.3	13.01	13.01	13.04
	SW_{11}	76.31	51.18	74.75	51.6	76.15	50.56	15.21	15.21	15.37
	SW_{12}	116.08	51.67	117.86	57.9	116.41	53.63	19.7	19.7	19.56
Total		1259.7	697.5	1318.7	733.1	1292.1	715.8	225.0	225.0	222.6

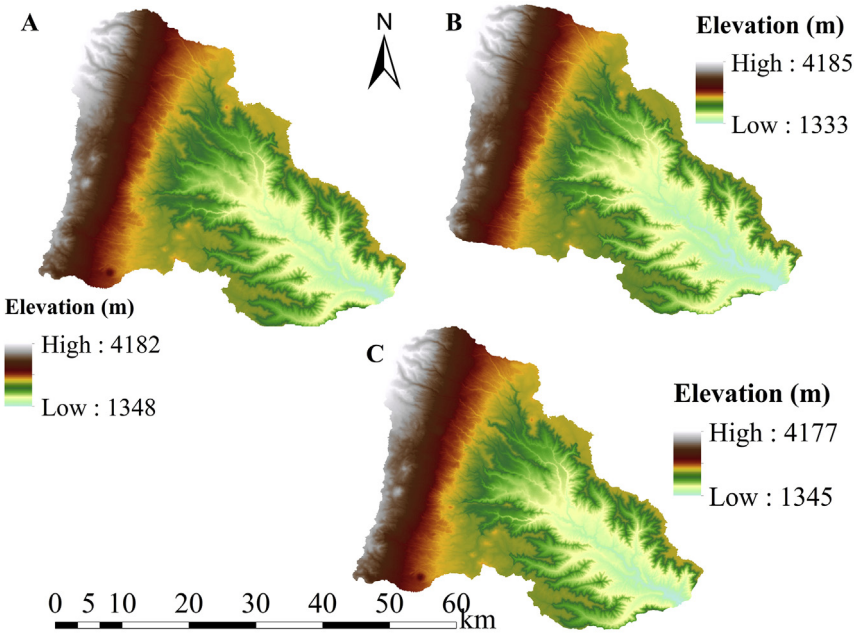

Figure 3. Digital elevation models (DEMs) of the study area: (A) SRTM, (B) ALOS, and (C) ASTER.

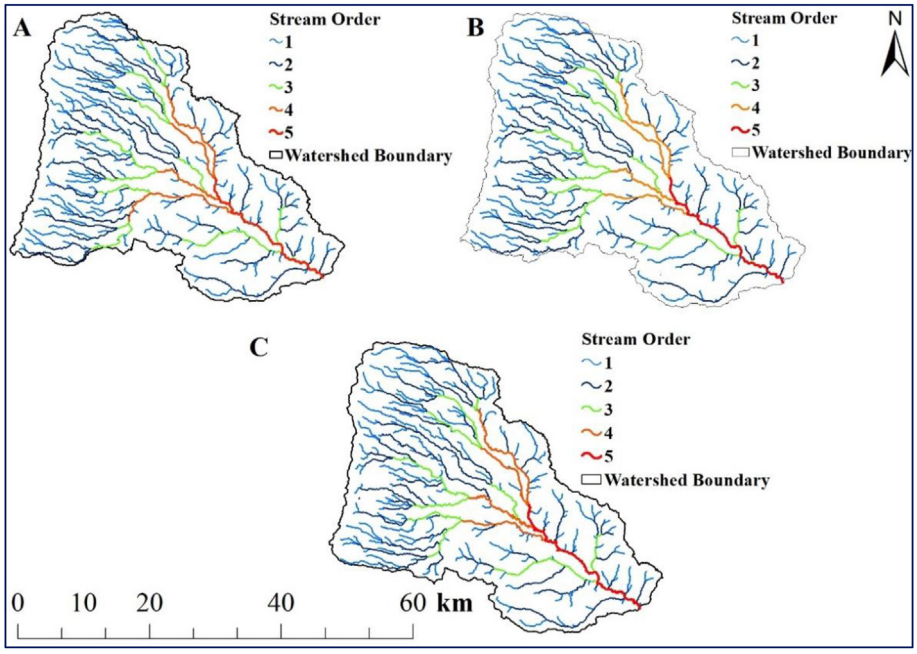

Figure 4. Stream orders of the Tena watershed: (A) ASTER, (B) SRTM, and (C) ALOS.

presented in Figure 7 characterize the risk of erosion, flooding, and sedimentation (Bhatt and Ahmed, 2014 and Alqahtani and Qaddah, 2019).

The morphometric parameters depicted in Table 3 express watershed physical characteristics. The Overland Flow (L_o) value is related to the movement of water on the land surface towards its confluence, termed the outlet, and has an inverse relation with the drainage density of the watershed. The lower the L_o value, the higher the travel time of the runoff. The D_t value relates to the soil, vegetation cover, climate, and infiltration capacity of the watershed, while D_i determines the rate movement of water through the soil profile. A sub-watershed with low D_t and D_i values is assumed to be affected by flooding, erosion, and landslides.

In this study, sub-watershed L_o is approximately equal, with maximum lengths for SW_1 and SW_2 returned by all DEM types (Table 3). In the Tena watershed the minimum value of L_o is reported for SW6, which implies that the fastest overland flow is observed at this sub-watershed (Table 3). D_t and D_i are highest for SW_{12} among the Tena

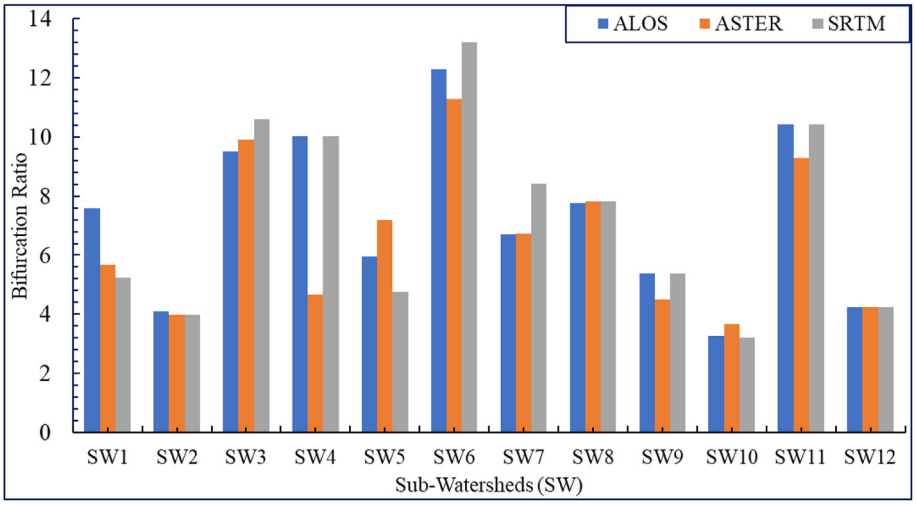

Figure 5. Relationship between DEMs and the bifurcation ratio of the Tena watershed.

Sub-Watersheds	p_{ALOS}	p_{ASTER}	p_{SRTM}	Fs_{ALOS}	Fs_{ASTER}	Fs_{SRTM}	Dd_{ALOS}	Dd_{ASTER}	Dd_{SRTM}
SW-1	0.09	0.14	0.33	0.31	0.32	0.31	0.55	0.53	0.53
SW-2	0.26	0.24	0.35	0.31	0.30	0.30	0.54	0.54	0.53
SW-3	0.03	0.02	0.02	0.33	0.31	0.32	0.64	0.63	0.62
SW-4	0.14	0.36	0.19	0.36	0.37	0.36	0.91	0.90	0.83
SW-5	0.16	0.14	0.25	0.36	0.33	0.36	0.91	0.91	0.89
SW-6	0.09	0.10	0.11	0.40	0.35	0.40	1.05	1.06	0.98
SW-7	0.18	0.13	0.18	0.33	0.38	0.33	0.88	0.90	0.86
SW-8	0.17	0.16	0.21	0.34	0.35	0.35	0.85	0.88	0.82
SW-9	0.16	0.16	0.24	0.25	0.21	0.26	0.94	0.93	0.91
SW-10	0.42	0.25	0.44	0.44	0.32	0.40	0.91	0.93	0.91
SW-11	0.62	0.70	0.60	0.43	0.39	0.43	0.78	0.74	0.74
SW-12	0.16	0.16	0.24	0.39	0.38	0.39	0.59	0.57	0.57

Low Value High Value

Figure 6. DEM sources and morphometric parameters linked to soil erosion, sedimentation, and runoff in the Tena watershed.

sub-watersheds (Table 3). Generally, $SRTM_{30m}$ is well suited to study runoff, while $ALOS_{30m}$ may produce satisfactory results when used to study soil erosion and flood assessment for the Tena watershed.

The compactness coefficient (C_c), Lemniscate's ratio (K), form factor (F_f), circulatory ratio (R_c), elongation ratio (R_e), and channel maintenance (C) are the most important morphometric parameters (Table 4). They are indirectly related to hydrologic, climatic, channel vegetation, and landform factors, and directly related to the shape of a watershed. For example, the minimum C value of a sub-watershed indicates a rapid travel time of water, with the rapid discharge of channel flow due to limited vegetation cover (Samal et al., 2015). In the present study area, high and low discharge speeds are observed at SW_6 and SW_1. For the further study of hydrologic characteristics, the $ALOS_{30m}$ and $ALOS_{30m}$ DEMs will be well suited. The circulatory ratio (R_c) ranges from 0.20 to 0.55 in the studied watershed, and within the range of Miller (1953) for SW_{12}, indicating that this sub-watershed features low runoff discharge and permeable soil chrematistics. Studies suggest that Rc is affected by stream length, stream frequency, and drainage pattern (Rai et al., 2014).

The morphometric parameter R_e, which is closely related to the slope and shape of the watershed, exhibits no significant difference in parameters between the three DEMs. As such, the Tena watershed is elongated (Schumm, 1956 and Table 4). The maximum and minimum values of F_f for the Tena watershed are 0.3 and 0.34 (Table 4). Meanwhile, sub-watersheds SW_1, SW_2, SW_3, SW_6, SW_8, and SW_{12} are characterized by lower peak flows due to their F_f values; while SW_{10} experiences a higher peak flow with shorter travel time (Table 4). The parameter Lemniscate's ratio (K) is at its maximum for SW_2 and minimum for SW_{10} for all DEM sources. The compactness coefficient (C_c) parameter depends on slope and is influenced by the perimeter of the watershed. Consequently, C_c is maximal for SW_9 according to all three DEMs (Table 4). Generally, the shape of the Tena watershed is considered as elongated, so that flow discharge reaches the outlet with a long travel time.

4. Conclusion

In this study, I used DEMs with identical resolution from different sources to identify the impacts of DEMs on morphometric parameters, through analyzing the Tena watershed. The results accomplished in this study take the form of morphometric basic and derived parameters, as reflected in the shape, length, stream network, and topography computed from $ASTER_{30m}$, $ALOS_{30m}$, and $SRTM_{30m}$ data. The results indicate that

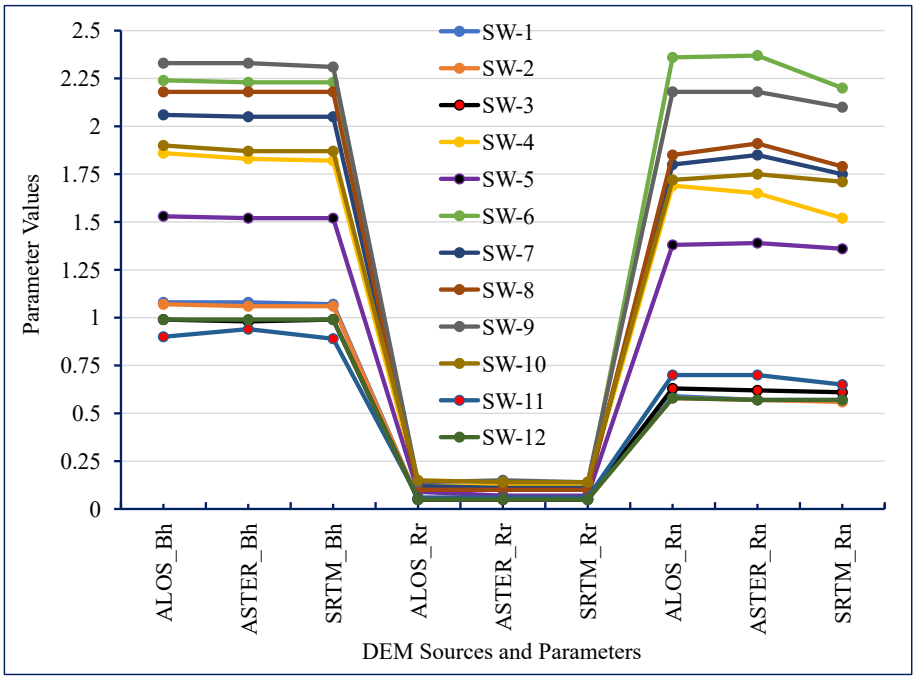

Figure 7. Relief aspects of the Tena watershed for the DEM sources: $ASTER_{30m}$, $SRTM_{30m}$, and $ALOS_{30m}$.

Table 3. Length of overland flow (L_o), drainage texture (D_t), and drainage intensity (D_i) of the Tena watershed.

DEM		ALOS	ASTER	SRTM	ALOS	ASTER	SRTM	ALOS	ASTER	SRTM
Parameters		L_o	L_o	L_o	D_t	D_t	D_t	D_i	D_i	D_i
Sub-Watersheds (SW)	SW1	0.91	**0.94**	**0.94**	0.54	0.56	0.53	0.56	0.60	0.58
	SW2	**0.93**	0.92	**0.94**	0.74	0.69	0.69	0.58	0.55	0.56
	SW3	0.78	0.80	0.81	0.67	0.60	0.67	0.51	0.49	0.52
	SW4	0.55	0.56	0.60	0.53	0.51	0.52	0.40	0.41	0.44
	SW5	0.55	0.55	0.56	0.67	0.73	0.76	0.40	0.36	0.40
	SW6	0.48	0.47	0.51	0.80	0.68	0.78	0.38	0.33	0.41
	SW7	0.57	0.55	0.58	0.60	0.69	0.59	0.38	0.42	0.38
	SW8	0.59	0.57	0.61	0.71	0.71	0.72	0.40	0.40	0.43
	SW9	0.53	0.54	0.55	0.30	0.24	0.30	0.27	0.22	0.28
	SW10	0.55	0.53	0.55	0.57	0.41	0.52	0.48	0.34	0.44
	SW11	0.64	0.68	0.68	0.64	0.56	0.65	0.55	0.52	0.59
	SW12	0.85	0.87	0.87	**0.87**	**0.78**	**0.84**	**0.66**	**0.66**	**0.68**

Table 4. Compactness coefficient (Cc), Lemniscate's ratio (K), form factor (Ff), circulatory ratio (Rc), elongation ratio (Re), and channel maintenance (C) of the Tena watershed.

DEM		ALOS						ASTER						SRTM					
Parameters		C	R_c	R_e	F_f	K	C_c	C	R_c	R_e	F_f	K	C_c	C	R_c	R_e	F_f	K	C_c
Sub-Watersheds (SW)	SW_1	1.83	0.29	0.62	0.30	0.84	1.86	1.87	0.28	0.62	0.30	0.84	1.87	1.89	0.28	0.62	0.30	0.84	1.90
	SW_2	1.85	0.49	0.61	0.30	0.85	1.44	1.84	0.47	0.61	0.30	0.85	1.46	1.89	0.46	0.61	0.30	0.85	1.47
	SW_3	1.56	0.45	0.62	0.30	0.82	1.50	1.59	0.40	0.62	0.30	0.83	1.58	1.62	0.46	0.62	0.30	0.83	1.48
	SW_4	1.10	0.36	0.64	0.32	0.77	1.66	1.11	0.33	0.64	0.32	0.77	1.74	1.20	0.34	0.64	0.32	0.77	1.71
	SW_5	1.10	0.45	0.63	0.31	0.80	1.49	1.10	0.44	0.61	0.30	0.85	1.51	1.12	0.45	0.62	0.30	0.83	1.49
	SW_6	0.95	0.43	0.62	0.30	0.82	1.53	0.94	0.40	0.62	0.30	0.82	1.57	1.02	0.41	0.62	0.30	0.82	1.56
	SW_7	1.14	0.41	0.63	0.31	0.80	1.57	1.11	0.39	0.63	0.31	0.81	1.60	1.17	0.40	0.63	0.31	0.81	1.58
	SW_8	1.18	0.38	0.61	0.30	0.85	1.63	1.14	0.36	0.61	0.30	0.85	1.67	1.22	0.36	0.61	0.30	0.85	1.67
	SW_9	1.07	0.21	0.64	0.32	0.78	2.17	1.07	0.20	0.64	0.32	0.78	2.23	1.10	0.21	0.64	0.32	0.78	2.21
	SW_{10}	1.10	0.37	0.65	0.34	0.75	1.64	1.07	0.37	0.65	0.34	0.75	1.65	1.09	0.36	0.65	0.34	0.75	1.66
	SW_{11}	1.28	0.37	0.64	0.32	0.78	1.65	1.35	0.35	0.64	0.32	0.77	1.68	1.36	0.37	0.64	0.32	0.78	1.63
	SW_{12}	1.69	0.55	0.62	0.30	0.82	1.35	1.74	0.44	0.62	0.30	0.82	1.50	1.75	0.51	0.62	0.30	0.82	1.40

$ASTER_{30m}$ is significantly better suited for to watershed analysis for hydrological investigation, including flood impacts, runoff, sediment, erosion, and watershed geometry analyses such as the compactness coefficient (C_c), Lemniscate's ratio (K), form factor (F_f), circulatory ratio (R_c), elongation ratio (R_e), and channel maintenance (C) when provided with similar morphometric parameters. More generally, the findings suggest that a specific type of DEM source should be used for design and analysis in further research.

Declarations

Author contribution statement

Tesfu Abebe Tesema: Conceived and designed the experiments; Performed the experiments; Analyzed and interpreted the data; Contributed reagents, materials, analysis tools or data; Wrote the paper.

Funding statement

This research did not receive any specific grant from funding agencies in the public, commercial, or not-for-profit sectors.

Data availability statement

Data will be made available on request.

Declaration of interests statement

The authors declare no conflict of interest.

Additional information

No additional information is available for this paper.

Acknowledgements

The author is very grateful to the anonymous reviewers and editor for their comments and critical suggestions that significantly helped improve the quality of the manuscript.

References

Abdeta, G.C., Tesemma, A.B., Tura, A.L., 2020. Morphometric analysis for prioritizing sub-watersheds and management planning and practices in Gidabo Basin, Southern Rift Valley of Ethiopia. Appl. Water Sci. 10, 158.

Ali, AMd, Solomatine, D.P., Di Baldassarre, G., 2015. Assessing the impact of different sources of topographic data on 1-D hydraulic modelling of floods. Hydrol. Earth Syst. Sci. 19, 631–643.

Alqahtani, F., Qaddah, A.A., 2019. GIS digital mapping of flood hazard in Jeddah-Makkah region from morphometric analysis. Arab J. Geosci. 12 (6), 199.

Aparna, P., Nigee, K., Shimna, P., Drissia, T.K., 2015. Quantitative analysis of geomorphology and flow pattern analysis of Muvattupuzha River Basin using Geographic Information system. J. Aquat. Proc. 4, 609–616 (2015).

Ariza-Villaverde, A.B., Jiménez-Hornero, F.J., Gutiérrez de Ravé, E., 2015. Influence of DEM resolution on drainage network extraction: a multifractal analysis. Geomorphology 241, 243–254.

Ayele, A., Yasuda, H., Shimizu, K., Nigussie, H., Kifle, W., 2017. Quantitative analysis and implications of drainage morphometry of the Agula watershed in the semi-arid northern Ethiopia. Appl. Wat. Sci. 7, 3825–3840.

Bayik, Caglar, Becek, K., Mekik, C., Ozendi, M., 2018. On the vertical accuracy of the ALOS world 3D-30m digital elevation model. Remote Sens. Lett. 9 (6), 607–615.

Bhatt, S., Ahmed, S.A., 2014. Morphometric analysis to determine floods in the Upper Krishna basin using Cartosat DEM. Geocarto Int. 29 (8), 878–894.

Burrough, P.A., 1986. Principles of Geographical Information Systems for Land Resource Assessment. Oxford University Press, New York.

Chorley, R.J., Malm, D.E.G., Pogorzelski, H.A., 1957. A new standard for estimating drainage basin shape. Am. J. Sci. 225, 138–141.

Choudhari, P.P., Nigam, Gaurav K., Singh, Sudhir Kumar, Thakur, Sapana, 2018. Morphometric based prioritization of watershed for groundwater potential of Mula river basin. Maharashtra, India, Geology, Ecology, and Landscapes 2 (4), 256–267.

Cook, A.J., Murray, T., Luckman, A., Vaughan, D.G., Barrand, N.E., 2012. A new 100-m digital elevation model of the Antarctic Peninsula derived from ASTER Global DEM: methods and accuracy assessment. Earth Syst. Sci. Data 4, 129–142.

Das, S., Patel, P.P., Sengupta, S., 2016. Evaluation of Different Digital Elevation Models for Analyzing Drainage Morphometric Parameters in a Mountainous Terrain: A Case Study of the Supin-Upper Tons Basin, Indian Himalayas. vol. 5. Springer Plus, p. 1544 (2016).

Dodov, B.A., Foufoula-Georgiou, E., 2006. Floodplain morphometry extraction from a high-resolution digital elevation model: a simple algorithm for regional analysis studies. Geosci. Rem. Sens. Lett. IEEE 3, 410–413.

Ekwueme, B.N., Agunwamba, J.C., 2020. Modeling the influence of meteorological variables on runoff in a tropical watershed. Civil Eng. J. 6, 2344–2351, 2020.

Evangelin, Ramani Sujatha, Selvakumar, R., Rajasimman, U.A.B., Victor, Rajamanickam G., 2015. Morphometric analysis of sub-watershed in parts of western ghats, south India using ASTER DEM, Geomatics. Nat. Haz. Risk 6 (4), 326–341.

Farhan, Y., 2017. Morphometric assessment of wadi wala watershed, southern Jordan using ASTER (DEM) and GIS. J GIS 9, 158–190.

Farhan, Y., Al-Shaikh, N., 2017. Quantitative Regionalization of W. Mujib-Wala sub-watersheds (Southern Jordan) using GIS and multivariate statistical techniques. Appl. Morph. Water. Manag. RS. GIS Multivar. Stat (Case Studies) 109, 149.

Farhan, Y., Nawaysa, S., 2015. Spatial assessment of soil erosion risk using RUSLE and GIS techniques. Environ. Earth Sci. 74, 4649–4669.

Farhan, Y., Anbar, A., Al-Shaikh, N., Mousa, R., 2017. Prioritization of semi-arid agricultural watershed using morphometric and principal component analysis, remote sensing, and GIS techniques, the Zerqa River Watershed. Norther. Jord. Agricult. Sci. 8, 113–148 (2017).

Ficklin, D.L., Stewart, I.T., Maurer, E.P., 2013. Effects of projected climate change on the hydrology in the Mono Lake Basin. Califor. Clim. Change 116 (1), 111–131.

Gebre, T., Kibru, T., Tesfaye, S., Taye, G., 2015. Analysis of watershed attributes for water resources management using GIS: the case of chelekot micro-watershed, tigray, Ethiopia. J. Geogr. Inf. Syst. 7, 177–190.

Ghumman, A.R., Al-Salamah, I.S., AlSaleem, S.S., Haider, H., 2017. Evaluating the impact of lower resolutions of digital elevation model on rainfall-runoff modeling for ungauged catchments. Environ. Monit. Assess. 189 (2), 54.

Gizachew, K., Berhan, G., 2018. Hydro-geomorphological characterization of Dhidhessa river basin, Ethiopia. Int. Soil Water Conserv. Res. 6, 175–183 (2018).

Guiamel, Ismail Adal, Lee, Han Soo, 2020. Watershed modelling of the Mindanao River Basin in the Philippines using the SWAT for water resource management. Civ. Eng. J. 6 (4), 626–648 (2020).

Gutema, D., Kassa, T., Sifan, A., Koriche, 2017. Morphometric analysis to identify erosion prone areas on the upper Blue Nile using GIS: case study of Didessa and Jema sub-basin, Ethiopia. Int. Res. J. Eng. Techn. 4 (8).

Her, Y., Frankenberger, J., Chaubey, I., Srinivasan, R., 2015. Threshold effects in HRU definition of the soil and water assessment tool. T ASABE 58, 367–378.

Horton, R.E., 1945. Erosional development of streams and their drainage basins; hydro-physical approach to quantitative morphology. Geol. Soc. Am. Bull. 56 (3), 275–370.

Ijam, A., Tarawneh, E., 2012. Assessing of sediment yield for wala dam catchment area in Jordan. Europ. Water 38, 43–58.

Jasmin, I., Mallikarjuna, P., 2013. Morphometric analysis of Araniar river basin using remote sensing and geographical information system in the assessment of groundwater potential. Arab J. Geosci. 6, 3683–3692.

Javed, A., Khanday, M.Y., Ahmed, R., 2009. Prioritization of sub-watershed based on morphometric and land use analysis using remote sensing and GIS techniques. J. Ind. Soc. Rem. Sens. 37, 261–274 (2009).

Jothimani, M., Dawit, Z., Mulualem, W., 2020. Flood susceptibility modeling of Megech river catchment, lake tana basin, north western Ethiopia, using morphometric analysis. Earth Syst. Environ.

Kaliraj, N., Chandrasekar, N., Magesh, S., 2015. Morphometric analysis of the river thamirabarani sub-basin in Kanya Kumari district, south west coast of Tamil nadu, India, using remote sensing and GIS. Environ. Earth Sci. 73, 7375–7401.

Kulkarni, M.D., 2013. The basic concept to study morphometric analysis of river drainage basin: a review. Int. J. Sci. Res. 4, 7 (2013).

Liebe, J., van de Giesen, N., Andreini, M., 2005. Estimation of small reservoir storage capacities in a semi-arid environment: a case study in the Upper East Region of Ghana. Phys. Chem. Earth, Parts A/B/C 30 (6), 448–454 (2005).

Lin, S., Jing, C., Chaplot, V., Yu, X., Zhang, Z., Moore, N., Wu, J., 2010. Effect of DEM resolution on SWAT outputs of runoff, sediment and nutrients. Hydrol. Earth Syst. Sci. 7 (4), 4411–4435.

McCullagh, P., 1978. Modern Concepts in Geomorphology (No. 6). Oxford University Press, Oxford.

Mesa, L.M., 2006. Morphometric analysis of a subtropical andean basin (Tucuma'n, Argentina). Environ. Geol. 50, 1235–1242.

Metz, M., Mitasova, H., Harmon, R.S., 2011. Efficient extraction of drainage networks from massive, radar-based elevation models with least cost path search. Hydrol. Earth Syst. Sci. 15, 667–678.

Miller, V.C., 1953. A Quantitative Geomorphologic Study of Drainage basin Characteristics in the Clinch Mountain Area, Virginia and Tennessee. Technical Report 3. Columbia University, New York.

Munoth, P., Goyal, R., 2019. Effects of DEM source, spatial resolution and drainage area threshold values on hydrological modeling. Water Resour. Manag. 33, 3303–3319.
Nardi, F., Vivoni, E.R., Grimaldi, S., 2006. Investigating a floodplain scaling relation using a hydrogeomorphic delineation method. Water Resour. Res. 42 (9), W09409.
Niyazi, B., Zaidi, S., Masoud, M., 2019. Comparative Study of Different Types of Digital Elevation Models on the Basis of Drainage Morphometric Parameters (Case Study of Wadi Fatimah Basin, KSA). Earth Syst. Environ. 3, 539–550 (2019).
Pande, C.B., Moharir, K., 2017. GIS based quantitative morphometric analysis and its consequences: A case study from Shanur River Basin, Maharashtra India. Appl. Wat. Sci. 7, 861 871 (2017).
Patton, P., Baker, V., 1976. Morphometgry and Floods in Small Drainage Basins Subject of Diverse Hydrogeomorphic Controls. Water Resour. Res. 12, 941–952.
Prakash, K., Singh, S., Shukla, U.K., 2016. Morphometric changes of the Varuna river basin, Varanasi district, Uttar Pradesh. J. Geom. 10 (1) (2016).
Prasad, R., Mondal, N., Banerjee, P., Nandakumar, M., Singh, V., 2008. Deciphering Potential Groundwater Zone in Hard Rock through the Application of GIS. Environ. Geol. 55, 467–475.
Rai, P.K., Mohan, K., Mishra, S., Ahmad, A., Mishra, V.N., 2014. A GISbased Approach in Drainage Morphometric Analysis of Kanhar River Basin. Appl Water Sci, India.
Rakesh, K., Lohani, A.K., Sanjay, K., Chatterjee, C., Nema, R.K., 2000. GIS based morphometric analysis of Ajay river basin upto Srarath gauging site of South Bihar. J. Appl. Hydrol. 14 (4), 45–54.
Sahu, N., Reddy, G.O., Kumar, N., Nagaraju, M.S.S., Srivastava, R., Singh, S.K., 2017. Morphometric analysis in basaltic Terrain of Central India using GIS techniques: a case study. Appl. Water Sci. 7 (5), 2493–2499.
Samal, D.R., Gedam, S.S., Nagarajan, R., 2015. GIS based drainage morphometry and its influence on hydrology in parts of Western Ghats region, Maharashtra, India. Geocarto Int. 30 (7), 755–778.
Sampson C., C., Smith M., A., Bates D., P., Neal C., J., Alfieri, L., Freer E., J., 2015. A high-resolution global flood hazard model. Water Resour. Res. 51, 7358–7381.
Schumann, G., Matgen, P., Cutler, M.E.J., Black, A., Hoffmann, L., Pfister, L., 2008. Comparison of remotely sensed water stages from LiDAR, topographic contours and SRTM. ISPRS J. Photogrammetry Remote Sens. 63 (3), 283–296.
Schumm, S.A., 1956. Evaluation of drainage system and slopes in badlands at Perth Amboy, New Jersey. Geol. Soc. Am. Bull. 67 (5), 597–646.
Sefercik, U.G., Alkan, M., 2009. Advanced analysis of differences between C and X Bands using SRTM data for mountainous topography. J. Indian Soc. Remote. Sens. 37, 335–349.
Sethupathi, A.S., Lakshmi Narasimhan, C., Vasanthamohan, V., Mohan, S.P., 2011. Prioritization of mini watersheds based on morphometric analysis using remote sensing and GIS in a drought prone Bargur Mathur sub-watersheds, Ponnaiyar River basin, India. Int. J. Geomatics Geosci. 2 (2), 403–414.
Singh, P., Gupta, A., Singh, M., 2014. Hydrological inferences from watershed analysis for water resource management using remote sensing and GIS techniques. Egypt J. Rem. Sens. Space Sci. 17, 111–121 (2014).
Soni, S., 2017. Assessment of morphometric characteristics of Chakrar watershed in Madhya Pradesh India using geospatial technique. Appl. Wat. Sci. 7, 2089–2102 (2017).
Sreedevi, P.D., Subrahmanyam, K., Ahmed, S., 2005. The significance of morphometric analysis for obtaining groundwater potential zones in a structurally controlled terrain. Environ. Geol. 47 (3), 412–420.
Strahler, A.N., 1952. Hypsometric analysis of erosional topography. Bull. Geol. Soc. Am. 63, 1117–1142.
Takaku, J., Tadono, T., Tsutsui, K., 2014. Generation of high-resolution global DSM from ALOS PRISM. In: The International Archives of the Photogrammetry, Remote Sensing and Spatial Information Sciences, Xl-4, pp. 243–248.
Tan, M.L., Ramli, H.P., Tam, T.H., 2018. Effect of DEM Resolution, Source, Resampling Technique and Area Threshold on SWAT Outputs. Water Resour. Manag. 32, 4591–4606 (2018).
Vaze, J., Teng, J., Spencer, G., 2010. Impact of DEM accuracy and resolution on topographic indices. Environ. Model. Software 25 (10), 1086–1098.
Waiyasusri, K., Chotpantarat, S., 2020. Watershed Prioritization of Kaeng Lawa Sub-Watershed, Khon Kaen Province Using the Morphometric and Land-Use Analysis: A Case Study of Heavy Flooding Caused by Tropical Storm Podul. Water 12, 1570.
Weydahl, D.J., Sagstuen, J., Dick, O.B., Ronning, H., 2007. SRTM DEM accuracy over vegetated areas in Norway. Int. J. Rem. Sens. 28 (16), 3513–3527.
Williams, W.A., Jensen, M.E., Winne, J.C., Redmond, R.L., 2000. An automated technique for delineating and characterizing valley-bottom settings Environ. Monit. Assess. 64, 105–114.
Woodrow, K., Lindsay B., J., Berg A., A., 2016. Evaluating DEM conditioning techniques, elevation source data, and grid resolution for field-scale hydrological parameter extraction. J. Hydrol. 540, 1022–1029.
Zhang, P., et al., 2014. Uncertainty of SWAT model at different DEM resolutions in a large mountainous watershed. Water Res. 53, 132–144.